RESEARCH ARTICLE OPEN ACCESS

The CADA-MRIT

An MRI Inventory Tool for Evaluating Cerebral Lesions in CADASIL Across Cohorts

Ruiting Zhang, MD, PhD, Chih-Hao Chen, MD, PhD, Sophie Tezenas Du Montcel, MD, PhD, Jessica Lebenberg, PhD, Yu-Wen Cheng, MD, PhD, Martin Dichgans, MD, PhD, Sung-Chun Tang, MD, PhD, and Hugues Chabriat, MD, PhD

Correspondence
Dr. Chabriat
hugues.chabriat@aphp.fr

Neurology® 2023;101:e1665-e1677. doi:10.1212/WNL.0000000000207713

Abstract

Background and Objectives

Cerebral autosomal dominant arteriopathy with subcortical infarcts and leukoencephalopathy (CADASIL) is the most frequent genetic cerebrovascular disease. The clinical aspects of the disease in relation to the various types of lesions on MRI vary widely not only within families but also between different cohorts reported worldwide. Many limitations prevent comparison of imaging data obtained with different scanners and sequences in different patient cohorts. We aimed to develop and validate a simple tool to inventory quickly the key MRI features in CADASIL to compare imaging data across different populations.

Methods

The Inventory Tool (CADA-MRIT) was designed by consensus after repeated expert meetings. It consists of 11 imaging items to assess periventricular, deep, and superficial white matter hyperintensity (WMH), lacunes, cerebral microbleeds (CMB), centrum semiovale and basal ganglia dilated perivascular spaces (dPVS), superficial and deep atrophy, large infarcts, and macrobleeds. The reliability, clinical relevance, and time-effectiveness of CADA-MRIT were assessed using data from 3 independent patient cohorts.

Results

Imaging data from 671 patients with CADASIL (440 from France, 119 from Germany, and 112 from Taiwan) were analyzed. Their mean age was 53.4 ± 12.2 years, 54.5% were women, 56.2% had stroke, and 31.1% had migraine with aura. Any lacune was present in at least 70% of individuals, whereas CMB occurred in 83% of patients from the Asian cohort and in only 35% of European patients. CADA-MRIT scores obtained for WMH, CMB, and dPVS were comparable regardless of the scanner or sequence used (weighted $\kappa > 0.60$). Intrarater and interrater agreements were from good to very good (weighted $\kappa > 0.60$). Global WMH and atrophy scores correlated strongly with accurate volumetric quantification of WMH or brain parenchymal fraction (Pearson $r > 0.60$). Different imaging scores were significantly associated with the main clinical manifestations of the disease. The time for evaluating 1 patient was approximately 2–3 minutes.

Discussion

The CADA-MRIT is an easy-to-use tool for analyzing and comparing the most frequent MRI lesions of CADASIL across different populations. This instrument is reliable. It can be used with different imaging sequences or scanners. It also provides clinically relevant scores in a very short time for completion.

From the Paris-Cité University (R.Z., J.L., H.C.), Inserm U1141 NeuroDiderot, France; Department of Radiology (R.Z.), the Second Affiliated Hospital of Zhejiang University, School of Medicine, Hangzhou, China; Department of Neurology (C.-H.C., Y.-W.C., S.-C.T.), National Taiwan University Hospital, Taipei; Department of Clinical Neurosciences (C.-H.C.), University of Calgary, Alberta, Canada; Sorbonne Université (S.T.D.M.), Paris Brain Institute, INSERM, INRIA, CNRS, APHP; Lariboisière University Hospital (J.L., H.C.), APHP, Translational Neurovascular Centre and Department of Neurology, Reference Center for Rare Vascular Diseases of the Central Nervous System and the Retina (CERVCO), FHU NeuroVasc, Paris, France; Department of Neurology (Y.-W.C.), National Taiwan University Hospital Hsinchu Branch; Institute for Stroke and Dementia Research (M.D.), University Hospital, Ludwig Maximilian University, Munich; German Center for Neurodegenerative Diseases (DZNE) (M.D.), Munich; and Munich Cluster for Systems Neurology (SyNergy) (M.D.), Germany.

Go to Neurology.org/N for full disclosures. Funding information and disclosures deemed relevant by the authors, if any, are provided at the end of the article.

The Article Processing Charge was funded by the authors.

Glossary

BG = basal ganglia; **BPF** = brain parenchymal fraction; **CADASIL** = cerebral autosomal dominant arteriopathy with subcortical infarcts and leukoencephalopathy; **CMB** = cerebral microbleed; **CSO** = centrum semiovale; **CSVD** = cerebral small vessel disease; **dPVS** = dilated perivascular space; **FLAIR** = fluid-attenuated inversion recovery; **MMSE** = Mini-Mental State Examination; **mRS** = modified Rankin scale; **NOTCH3** = neurogenic locus notch homolog protein 3; **SWI** = susceptibility-weighted imaging; **WMH** = white matter hyperintensities.

Introduction

Cerebral autosomal dominant arteriopathy with subcortical infarcts and leukoencephalopathy (CADASIL) is the most common inherited cause of stroke and vascular dementia.[1] It is a severe condition that progresses with age,[2] and its clinical worsening varies widely between affected individuals.[3,4] The origin of this variability is partly related to the location of the sequence variant in the neurogenic locus notch homolog protein 3 (*NOTCH3*) gene[5,6] or to the presence of cerebrovascular risk factors[7,8] but remains largely undetermined. The extent of characteristic cerebral lesions of the disease and their distribution are undoubtedly central to this variability.[3,9] Thus, understanding the variability of MRI signal changes and their determinants at a large scale not only within families but also between large CADASIL cohorts is crucial to improve prediction of clinical course and develop future clinical trials.

Regarding brain imaging to date, comparative studies between cohorts remain rare and are only based on historical data from the literature.[10,11] This is mainly because quantitative imaging studies are extremely difficult to perform for rare diseases, particularly in a routine clinical setting and when MRI data have been collected over many years. In addition, some pitfalls encountered in the automatic segmentation of MRI lesions in CADASIL have not yet been fully resolved, such as the difficulty of separating certain white matter lesions of variable signal in close contact with the cerebral cortex[12] or the isolation of lacunes from the frequent dilated perivascular spaces (dPVS). Moreover, while the segmentation of white matter hyperintensities (WMH) has benefited from extensive research efforts supported by medical image computing societies,[13] the automatic segmentation of lacunes, microbleeds, or PVS is still being studied and is far from being considered a valid method to evaluate heterogeneous and variable imaging findings, as observed in patients with CADASIL.[14] Elsewhere, for analyzing imaging data from multiple cohorts, there are many other limitations to be overcome such as: (1) differences in imaging sequences or protocols across centers,[15-17] (2) modifications related to advances in imaging techniques or acquisitions over a long period of recruitment (1.5T MRI replaced by 3T or T2* replaced by susceptibility-weighted imaging [SWI]), (3) inconsistency between quantitative methods based on multiple algorithms or approaches,[18,19] (4) difficulties related to the cost for sharing original imaging data between centers in a reliable, secure, and anonymous way for a long time and within an ethical framework.

An alternative approach, especially for comparative cohort studies, could be to adopt already validated visual rating scales from the literature. Different tools were previously designed for rating MRI lesions related to sporadic cerebral small vessel disease (CSVD) in stroke patients or in the general population.[20-23] However, most of these instruments have been validated to specifically assess 1 category of lesions such as the Fazekas scale for WMH, the Global Cortex Atrophy scale for brain atrophy, or the Microbleed Anatomical Rating Scale for assessing the location and number of microbleeds.[24-26] Some of these scales were validated based on specific imaging protocols.[21,23] For other scales, such as the Fazekas scale whose maximal score is reached in more than half of patients with CADASIL, a ceiling effect was observed due to the early emergence of extensive WMH.[19,20,27] Finally, the assessment of specific CADASIL imaging features such as WMH in the anterior temporal lobes has never been considered.

In this study, we aimed to develop and validate a practical tool that could quickly inventory the key MRI features observed in CADASIL and could be used easily by clinicians and researchers to compare their data across multiple patient populations even when studied with different MRI scanners and sequences.

Methods

Data Collection Methods

Patients with CADASIL from 3 independent cohorts were included in this study. Details of these cohorts have been already reported.[9,28,29] In brief, consecutive patients with CADASIL who were at least 18 years of age were evaluated at Lariboisière hospital (cohort 1), Ludwig-Maximilians-Universität hospital (cohort 2), and National Taiwan University Hospital (cohort 3) between October 2003 and February 2021 (cohort 1), April 2003 and September 2010 (cohort 2), January 2019 and August 2022 (cohort 3). In all cases, the diagnosis was confirmed by genetic testing showing a typical sequence variant of *NOTCH3* altering the number of cysteine residues. Clinical and demographic data were collected by study investigators during inclusion. All enrolled patients underwent detailed baseline neurologic examination, including a brief evaluation of cognitive deficits with the Mini-Mental State Examination (MMSE) and degree of disability based on the modified Rankin scale (mRS).

Figure 1 CADASIL Imaging Inventory

The CADASIL MRI Inventory Tool (CADA-MRIT)

White matter hyperintensities (WMH)			
Periventricular WMH (PVH) [In contact with the ventricles]			
☐ 0 : Absence ☐ 1 : "Caps" or pencil-thin lining ☐ 2 : Smooth "halo" ☐ 3 : PVH extending into the deep white matter partly merging with deep WMH ☐ 4 : PVH extending into the deep white matter completely merging with deep WMH (PVH cannot be separated from deep WMH anywhere)			
Deep WMH [Between PVH and superficial WMH]			
☐ 0 : Absence ☐ 1 : Punctate foci ☐ 2 : Beginning confluence of foci ☐ 3 : Large confluent areas			
Superficial WMH [In contact with U fibers; Evaluate frontal and temporal pole white matter specifically, if different in the 2 locations, use the most severe one]			
☐ 0 : Absence ☐ 1 : Punctate foci ☐ 2 : Beginning confluence of foci ☐ 3 : Confluent WMH partly merging with deep WMH ☐ 4 : Confluent WMH completely merging with deep WMH			
Lacunes			
☐ 0 : 0	☐ 1 : 1-5	☐ 2 : 6-10	☐ 3 : >10
Cerebral microbleeds (CMB)			
☐ 0 : 0	☐ 1 : 1-5(T2*)/1-10(SWI)	☐ 2 : 6-10(T2*)/11-20(SWI)	☐ 3 : >10(T2*)/>20(SWI)
Dilated perivascular spaces (dPVS) *[Count in the slice with the highest number. T1 – sum of both sides, and T2 – the higher score on one side]*			
Centrum semiovale (CSO)		*Basal ganglia*	
☐ 0 : <10		☐ 0 : <10	
☐ 1 : 10-20		☐ 1 : 10-20	
☐ 2 : >20		☐ 2 : >20, innumerable or status cribrosum	
Atrophy			
Superficial [Dilation of the sulcus; Evaluate central sulcus and lateral sulcus specifically, if different in the 2 locations, use the most severe one]		*Deep [Dilation of the lateral ventricles]*	
☐ 0 : Absence ☐ 1 : Mild ☐ 2 : Moderate ☐ 3 : Severe		☐ 0 : Absence ☐ 1 : Mild ☐ 2 : Moderate ☐ 3 : Severe	
Large infarct (>20mm)			
☐ 0 : 0	☐ 1 : 1	☐ 2 : >1	
Macrobleeds (>15mm)			
☐ 0 : 0	☐ 1 : 1	☐ 2 : >1	

The Items and scores composing the imaging inventory tool are presented on a single page sheet.

As in the previous study, we defined disability as mRS ≥3.[9] MRI examination was performed on the same day of baseline neurologic examination in cohorts 1 and 2, and within 3 months after inclusion in cohort 3.

The MRI acquisition parameters and the quantification methods of imaging data are detailed in the eMethods section (links.lww.com/WNL/D93).

Standard Protocol Approvals, Registrations, and Patient Consents

Informed consent was obtained from each patient or a close relative if the patient was too severely disabled to give written consent. This study was approved by independent ethics committees (cohort 1: updated agreement CEEI-IRB-17/388; cohort 2: the Ludwig Maximilian University medical faculty, No. 299/03; cohort 3: National Taiwan University Hospital: No. 201807044RIND) in all participating centers and conducted in accordance with the Declaration of Helsinki.

Design of the Inventory Tool

The different items composing the inventory tool were prepared after 4 working zoom meetings of 2–3 hours between the authors. The selection of the different items was established by consensus after repeated discussion and tests so that the final scale would be: (1) easy to use, (2) quick to assess, (3) usable on the MRI sequences most commonly used in clinical practice for patients with CADASIL, (4) usable to summarize all lesion features currently observed in the disease (e.g., WMH in the temporal lobes), (5) able to capture the differences between cohorts (frequent hemorrhagic lesions in Asian and ischemic lesions in European patients), (6) sensitive to the extension and number of lesions from the beginning to the late stage of the disease, and (7) simple and as conservative as possible by adapting items already proposed in previous validated scales.

The final inventory included 11 items for evaluating the different lesions using the STRIVE criteria: (1) periventricular WMH (PVH), (2) deep WMH, (3) superficial WMH, (4)

Figure 2 WMH, Lacune, CMB, dPVS, and Atrophy Scores From the Inventory Tool

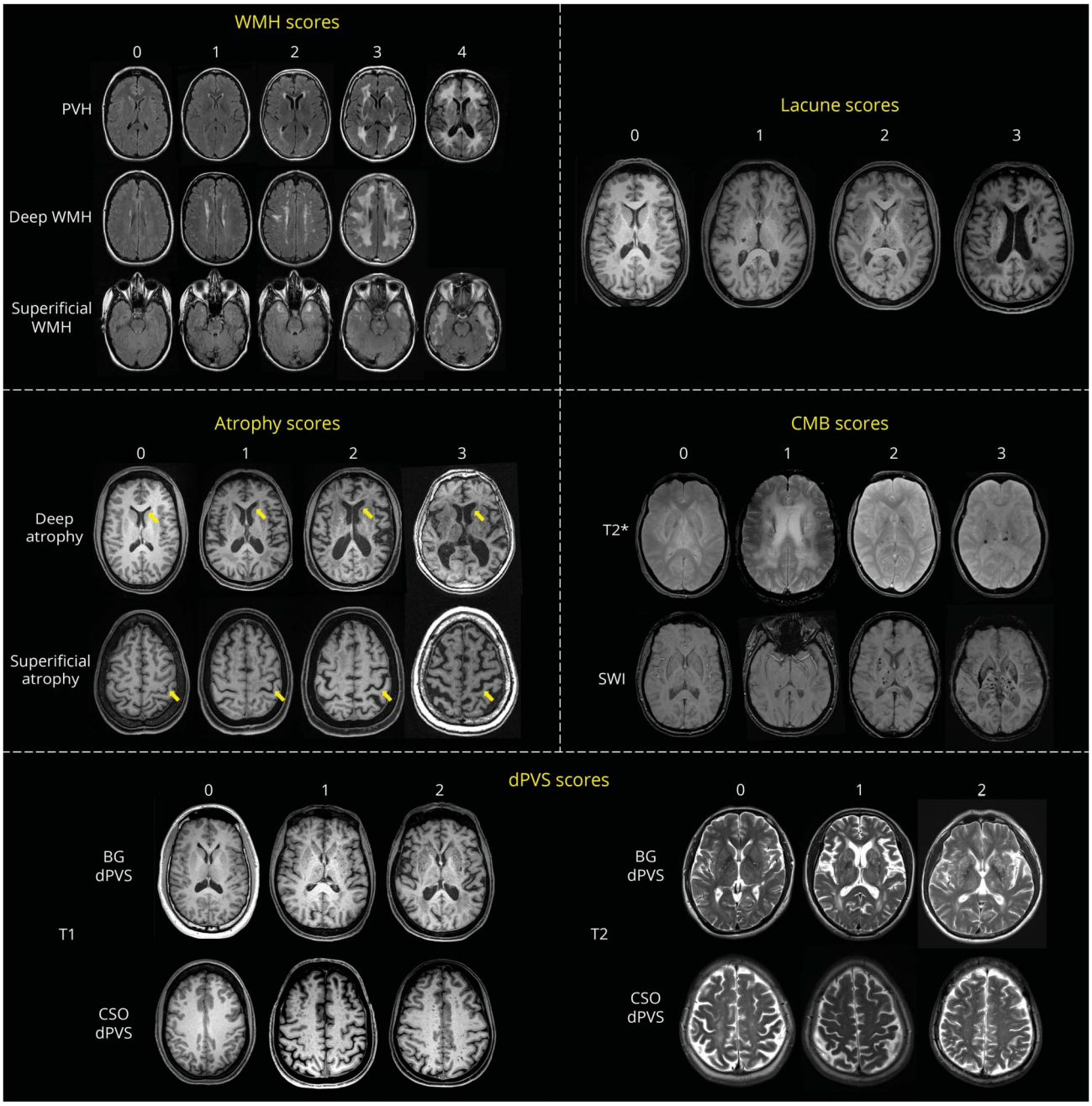

The different scores obtained from the imaging inventory tool are presented with the corresponding images to facilitate their interpretation. BG = basal ganglia; CMB = cerebral microbleed; CSO = centrum semiovale; dPVS = dilated perivascular space; PVH = periventricular WMH; SWI = susceptibility-weighted imaging; WMH = white matter hyperintensity.

lacunes, (5) cerebral microbleeds (CMB), (6–7) dPVS in the centrum semiovale (CSO) or in basal ganglia (BG), (8) superficial atrophy, (9) deep atrophy, (10) large infarcts, and (11) macrobleeds (Figure 1). The levels of each item were chosen according to the literature, the distribution of data in different subsamples including extreme cases observed in the different cohorts, and the long clinical experience of some authors (H.C., S.-C.T.). The final scoring adopted by consensus is illustrated in Figure 2. The method used for building the scoring system is detailed in eMethods (links.lww.com/WNL/D93).

Assessment and Validation of the Inventory Tool

To validate the inventory tool, we look for (1) the agreement between the scoring obtained from different MR protocols, (2) the interrater and intrarater agreement of the composing scores, and (3) the external validity through the correlation between some items and quantitative lesions measures. The clinical correlates of items derived from the inventory tool and its time-effectiveness were also assessed. This validation procedure was based on

Table 1 Demographic and Clinical Characteristics of the Cohorts

	Cohort 1 (n = 440)	Cohort 2 (n = 119)	Cohort 3 (n = 112)
Age, y, mean ± SD	52.4 ± 12.0	48.3 ± 9.9	62.5 ± 10.6
Sex, female, n (%)	244 (55.5)	69 (58.0)	53 (47.3)
Education level,[a] median (IQR)	5 (4–7)	5 (4–5)	6 (5–7)
Stroke, n (%)	230 (52.3)	82 (68.9)	65 (58.0)
Migraine with aura, n (%)	163 (37.0)	45 (37.8)	1 (0.9)
Disability, n (%)	66 (15.1)	12 (10.1)	24 (21.4)
MMSE, median (IQR)	28 (26–30)	29 (27–30)	28 (24–29)
Normalized WMH fraction, %, median (IQR)	3.3 (1.8–5.9)	5.7 (3.7–10.4)	2.4 (1.2–3.7)
Lacune number, median (IQR)	5 (1–13)	3 (0–7)	3 (1–9)
CMB number, median (IQR)	0 (0–2)	0 (0–1)	9 (2–30)
BPF, %, median (IQR)	82.6 (78.6–85.0)	88.1 (84.3–90.9)	72.2 (68.9–75.5)

Abbreviations: BPF = brain parenchymal fraction; CMB = cerebral microbleed; IQR = interquartile range; MMSE = Mini-Mental State Examination; WMH = white matter hyperintensities.
[a] Education level: 7 levels according to the number of education years. Level 1 = 0; level 2 = 1–5; level 3 = 6–8; level 4 = 9; level 5 = 10–11; level 6 = 12; level 7 = over 12 years.

different results obtained by 4 experienced raters (a neuroradiologist—R.Z. [rater 1] and 3 neurologists—C.-H.C. [rater 2], H.C. [rater 3]; Y.-W.C. [rater 4]) with 6–35 years of experience in clinical and imaging research on CSVD. Analysis was performed using fully anonymized MRIs from the different cohorts and blinded to the clinical status of all individuals.

Agreement Between Scoring Obtained From Different MR Acquisition Protocols

The scores obtained from the inventory tool were compared when images were from a basic or an advanced MRI protocol. More specifically, the agreement between WMH scores obtained with 3D or 2D fluid-attenuated inversion recovery (FLAIR) images, CMB scores obtained with T2* or SWI, or dPVS scores obtained with T1-weighted or T2-weighted images was analyzed. For WMH, 40 randomly selected 3D FLAIR images from cohort 1 were resampled to 2D FLAIR images, and then, the original 3D images and the 2D images resampled from the 3D images were evaluated by rater 1 during 2 separate sessions at 4 weeks interval. Similarly, for CMB, data from 83 patients from cohort 1 who had both SWI and T2* images were also analyzed by rater 1 in 2 separate 4-week sessions. For dPVS, 40 patients having had both T1-weighted and T2-weighted images from cohort 3 were randomly selected and analyzed by rater 2 in 2 separate additional sessions. The agreement between the different imaging protocols was analyzed for each inventory item using the linear weighted κ measure of agreement. The weighted κ results were interpreted as poor (0–0.20), fair (0.21–0.40), moderate (0.41–0.60), good (0.61–0.80), or very good (0.81–1) agreement.[30]

Intrarater and Interrater Agreements for the Different Inventory Items

Forty patients with a basic MRI protocol (2D FLAIR, low-resolution 3D T1, T2*) and 40 others with an advanced MRI protocol (3D FLAIR, high-resolution 3D T1, SWI) were randomly selected from cohort 1 among 440 patients by age of distribution in 10-year intervals. Images were then displayed using the ITK-SNAP 3.0 software (Cognitica, Philadelphia, PA) and assessed both by rater 1 and rater 3. Rater 1 also analyzed the same data a second time after a 4-week interval. Each rater was blinded to the other rater's ratings. Before these independent rating sessions, the 2 raters had together training sessions on 10 randomly selected patients, and cases of disagreement were solved by discussion. Appropriate guidance for using the inventory tool was prepared based on this experience.

For additional validation, 40 patients were also randomly selected from cohort 3 and assessed by rater 2 and rater 4 separately. Similarly, 40 patients were randomly selected from cohort 2 and assessed twice by rater 1 for intra-rater agreement. We also built a mixed database with 14 patients from cohort 1, 13 patients from cohort 2, and 13 patients from cohort 3, who were randomly selected from the 3 cohorts. The mixed imaging database was then assessed by rater 1 and rater 2 for interrater agreement. Intrarater and interrater agreements were calculated using the linear weighted κ measure of agreement.

Correlations Between the Items From the Inventory Tool and Quantification of Lesions

We studied the correlations between the different WMH items. We also looked at the relationship between the total

Table 2 Distribution of the Different Scores of the Inventory in the 3 Cohorts

	Cohort 1 (n = 440)	Cohort 2 (n = 119)	Cohort 3 (n = 112)
PVH, n (%)			
0	4 (0.9)	0 (0)	1 (0.9)
1	26 (5.9)	4 (3.4)	12 (10.7)
2	140 (31.8)	20 (16.8)	24 (21.4)
3	187 (42.5)	69 (58.0)	57 (50.9)
4	83 (18.9)	26 (21.8)	18 (16.1)
Deep WMH, n (%)			
0	3 (0.7)	2 (1.7)	6 (5.4)
1	48 (10.9)	11 (9.2)	11 (9.8)
2	74 (16.8)	19 (16.0)	33 (29.5)
3	315 (71.6)	87 (73.1)	62 (55.4)
Superficial WMH, n (%)			
0	30 (6.8)	10 (8.4)	85 (75.9)
1	177 (40.2)	21 (17.6)	17 (15.2)
2	87 (19.8)	30 (25.2)	4 (3.6)
3	95 (21.6)	37 (31.1)	3 (2.7)
4	51 (11.6)	21 (17.6)	3 (2.7)
Lacune, n (%)			
0	126 (28.6)	26 (21.8)	21 (18.8)
1	123 (28.0)	33 (27.7)	51 (45.5)
2	79 (18.0)	19 (16.0)	24 (21.4)
3	112 (25.5)	41 (34.5)	16 (14.3)
CMB, n (%)			
0	281 (63.9)	80 (67.2)	19 (17.0)
1	95 (21.6)	21 (17.6)	37 (33.0)
2	28 (6.4)	10 (8.4)	14 (12.5)
3	36 (8.2)	8 (6.7)	42 (37.5)
BG dPVS, n (%)[a]			
0	142 (32.3)	50 (42.0)	15 (13.4)
1	247 (56.1)	65 (54.6)	35 (31.3)
2	47 (10.7)	3 (2.5)	62 (55.4)
CSO dPVS, n (%)[a]			
0	235 (53.4)	78 (65.5)	60 (53.6)
1	150 (34.1)	31 (26.1)	32 (28.6)
2	51 (11.6)	9 (7.6)	20 (17.9)
Superficial atrophy, n (%)			
0	290 (65.9)	98 (82.4)	20 (17.9)
1	89 (20.2)	18 (15.1)	45 (40.2)
2	57 (13)	2 (1.7)	32 (28.6)
3	4 (0.9)	1 (0.8)	15 (13.4)
Deep atrophy, n (%)			
0	279 (63.4)	77 (64.7)	29 (25.9)
1	101 (23)	29 (24.4)	42 (37.5)
2	48 (10.9)	9 (7.6)	30 (26.8)
3	12 (2.7)	4 (3.4)	11 (9.8)
Large infarct, n (%)			
0	429 (97.5)	116 (97.5)	109 (97.3)
1	10 (2.3)	3 (2.5)	3 (2.7)
2	1 (0.2)	0 (0)	0 (0)
Macrobleeds, n (%)			
0	427 (97.0)	119 (100)	84 (75.0)
1	9 (2.0)	0 (0)	21 (18.8)
2	4 (0.9)	0 (0)	7 (6.3)

Abbreviations: BG = basal ganglia; CMB = cerebral microbleed; CSO = centrum semiovale; dPVS = dilated perivascular spaces; PVH = periventricular WMH; WMH = white matter hyperintensities.
[a] dPVS were evaluated in 436 patients in cohort 1, 118 patients in cohort 2, and 112 patients in cohort 3. Four patients in cohort 1 and 1 patient in cohort 2 were excluded because of severe artifact on T1-weighted images.

WMH score obtained as the sum of the 3 different WMH items and the quantitative measure of WMH calculated in the whole brain. Similarly, we studied the correlation between the different atrophy items. The sum of the 2 atrophy items was also compared with the brain parenchymal fraction (BPF). For this purpose, first, we transformed the data to follow a normal distribution using cube (normalized WMH fraction) or quantile transformation (BPF). Then, the Pearson correlation between the inventory tool items and the respective quantification lesion was computed. We also used scatterplots to show the correlation between these scores and their respective quantitative measurements.

Association Between the Inventory Tool Items and the Main Clinical Features of the Disease

To address the clinical value of the different items derived from the inventory tool, we combined the 3 cohorts (n = 671 individuals) and assessed their association with the past occurrence of stroke (ischemic and hemorrhagic), attacks of migraine with aura, degree of disability (mRS < or ≥3), and MMSE score. Multivariable logistic (stroke, migraine with aura, disability) or linear model (MMSE), adjusted for age and sex, were used. Additional adjustment for the level of

Figure 3 Relationships Between the Total WMH Score (Sum of Periventricular and Deep and Superficial WMH Scores) and the Volume of WMH and Between the Total Atrophy Score (Sum of Deep and Superficial Atrophy Scores) and the Brain Parenchymal Fraction

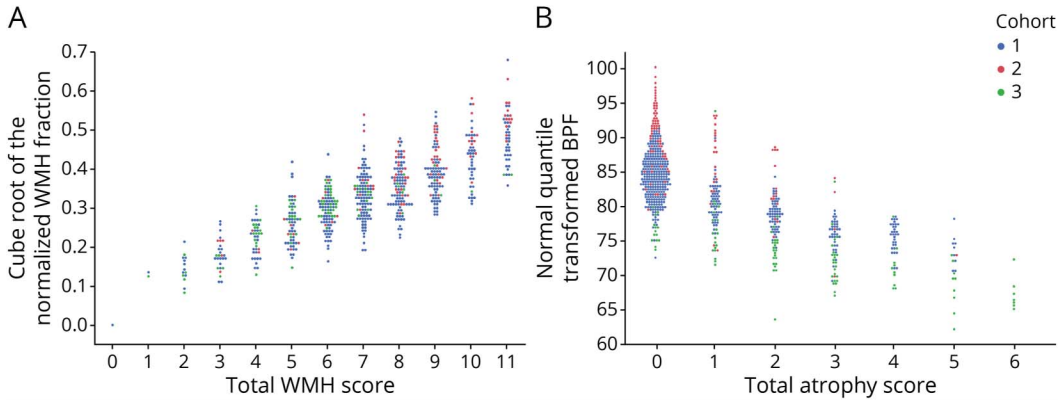

Scatterplots showing (A) the significant association between the total WMH score and the cube root of normalized WMH fraction; (B) the significant association between the total atrophy score and the normal quantile-transformed BPF. BPF = brain parenchymal fraction; WMH = white matter hyperintensity.

education was considered for the association with MMSE. To test the association between clinical variables and each of the 11 inventory tool items, statistical significance was set at a probability value of <0.0045 (0.05/11, Bonferroni adjustment). To search for an independent association between the inventory tool scores and the different clinical features, multivariate regression analysis was performed with statistical significance set at a probability value of <0.05 (model 2: all imaging items included simultaneously in the model without selection). Finally, the models obtained after selecting the significant items from the CADA-MRIT for predicting each clinical outcome were compared with the predictive models obtained using a global score as the total CSVD score.[31] All analyses were performed by R version 3.6.2 or SPSS 22.0.

Time-Effectiveness

The time requested for evaluating MRIs using the inventory tool was recorded using a stopwatch in 80 patients from cohort 1 and 40 patients from cohort 3 (the same patients selected for intrarater and interrater analysis). Rater 1 and rater 2 recorded the time spent to fulfill each item of the inventory, while rater 3 recorded the time spent to complete the entire inventory.

Data Availability

Data that support the findings of this study are available from the corresponding author and coauthors (H.C., M.D., S.-C.T.) on reasonable request.

Results

Main Characteristics of Patients From the 3 Cohorts

The main demographic and clinical characteristics of the 671 patients from the 3 CADASIL cohorts are summarized (n = 440 from cohort 1, n = 119 from cohort 2, and n = 112 from cohort 3) in Table 1. The mean age of the whole population was 53.4 ± 12.2 years, 366 (54.5%) individuals were female, 377 (56.2%) had stroke, and 209 (31.1%) patients had a history of migraine with aura. Patients of cohort 3 (from Taiwan) included the oldest patients. In contrast with the other cohorts, migraine with aura was observed only in 1 individual in this cohort. The patients' imaging characteristics are summarized in Table 2. Any lacune was present in at least 71% (cohort 1) to 81% (cohort 3) of patients. CMB were present in 83% of patients in cohort 3 but in only 33%–36% in cohorts 1 and 2.

Agreements Between Scoring Obtained From Different MR Acquisition Protocols

Agreements between the different WMH scores obtained using the original 3D images and the 2D images resampled from the 3D images were very good (PVH: weighted κ = 0.939 [0.859–1.000]; deep WMH: weighted κ = 0.828 [0.650–0.961]; superficial WMH: weighted κ = 0.839 [0.727–0.926]). Agreement between CMB scores obtained with SWI and T2* images was very good (weighted κ = 0.848 [0.751–0.932]). Agreements between dPVS scores obtained using T1 and T2 were also good to very good (CSO dPVS: weighted κ = 0.811 [0.652–0.941]; BG dPVS: weighted κ = 0.631 [0.399, 0.824]).

Intrarater and Interrater Agreements for the Different Inventory Items

As summarized in eTable 1 (links.lww.com/WNL/D94) and 2, 80 of 88 intrarater and interrater agreements for the different inventory tool items were good or very good (weighted κ between 0.647 and 1.000). The 8 fair-to-moderate agreements included the interrater agreements for deep WMH from cohort 1 with advanced MRI protocol (weighted κ = 0.516), superficial atrophy from cohort 3 (weighted κ =

Table 3 Association Between the Different Inventory Tool Items and Different Clinical Outcomes

	Stroke, OR (95% CI)		Migraine with aura, OR (95% CI)		Disability, OR (95% CI)		MMSE, β (95% CI)	
	Model 1	Model 2	Model 1	Model 2	Model 1	Model 2	Model 1	Model 2
PVH	**2.167 (1.708–2.749)***	1.141 (0.801–1.625)	1.117 (0.881–1.417)	0.961 (0.661–1.396)	**4.305 (2.889–6.415)***	**2.208 (1.252–3.896)****	*−1.418 (−1.849 to −0.986)**	*−1.211 (−1.794 to −0.629)****
Deep WMH	**1.952 (1.523–2.502)***	1.173 (0.849–1.622)	1.432 (1.103–1.860)	1.303 (0.935–1.815)	**2.316 (1.321–4.060)***	0.766 (0.379–1.546)	0.006 (−0.459 to 0.470)	**0.928 (0.397 to 1.460)****
Superficial WMH	**1.301 (1.145–1.480)***	1.078 (0.904–1.285)	**1.355 (1.174–1.565)***	1.162 (0.964–1.402)	1.127 (0.959–1.324)	0.959 (0.753–1.221)	−0.029 (−0.276 to 0.217)	−0.121 (−0.405 to 0.163)
Total WMH	**1.271 (1.177–1.374)***	—	**1.160 (1.068–1.260)***	—	**1.267 (1.131–1.419)***	—	−0.160 (−0.305 to −0.016)	—
Lacune	**2.454 (2.042–2.950)***	**2.317 (1.854–2.895)*****	0.996 (0.841–1.179)	1.036 (0.833–1.288)	**2.759 (2.105–3.616)***	**2.271 (1.591–3.241)*****	*−0.835 (−1.144 to −0.526)**	−0.250 (−0.597 to 0.097)
CMB	**1.329 (1.112–1.588)***	0.958 (0.770–1.193)	*0.659 (0.526–0.826)**	*0.698 (0.536–0.909)***	**1.514 (1.232–1.861)***	1.175 (0.914–1.512)	*−0.674 (−1.013 to −0.335)**	−0.079 (−0.436 to 0.278)
CSO dPVS	*0.712 (0.567–0.894)**	0.881 (0.677–1.146)	1.104 (0.863–1.412)	1.144 (0.871–1.501)	*0.562 (0.386–0.817)**	0.885 (0.567–1.381)	**0.829 (0.388 to 1.270)***	0.337 (−0.092 to 0.765)
BG dPVS	1.068 (0.808–1.410)	1.063 (0.766–1.473)	0.756 (0.556–1.030)	0.904 (0.642–1.274)	1.045 (0.704–1.550)	0.860 (0.521–1.420)	−0.042 (−0.596 to 0.513)	0.216 (−0.318 to 0.750)
Total dPVS	0.859 (0.730–1.010)	—	0.959 (0.802–1.147)	—	0.776 (0.609–0.990)	—	**0.420 (0.100 to 0.741)**	—
Superficial atrophy	1.090 (0.851–1.396)	0.908 (0.643–1.282)	*0.363 (0.25–0.526)**	*0.344 (0.218–0.545)****	**2.570 (1.860–3.551)***	**1.581 (1.046–2.392)#**	*−1.886 (−2.346 to −1.426)**	*−1.145 (−1.697 to −0.592)****
Deep atrophy	1.290 (1.022–1.627)	0.861 (0.619–1.199)	0.787 (0.599–1.034)	**1.487 (1.024–2.159)#**	**2.926 (2.178–3.932)***	1.352 (0.910–2.009)	*−1.885 (−2.311 to −1.459)**	*−0.719 (−1.254 to −0.185)***
Total atrophy	1.120 (0.978–1.283)	—	*0.698 (0.583–0.834)**	—	**1.981 (1.646–2.384)***	—	*−1.215 (−1.462 to −0.968)**	—
Large infarct	**NA**	—	1.387 (0.520–3.697)	1.338 (0.474–3.776)	3.822 (1.468–9.951)	**3.158 (1.093–9.122)#**	−1.141 (−2.999 to −0.717)	−0.261 (−1.972 to 1.450)
Macrobleeds	2.136 (1.147–3.980)	**3.116 (1.534–6.332)****	0.196 (0.051–0.747)	0.372 (0.102–1.360)	1.822 (1.072–3.097)	**2.122 (1.062–4.239)#**	*−1.652 (−2.637 to −0.667)**	*−1.248 (−2.218 to −0.277)#*

Abbreviations: BG = basal ganglia; CMB = cerebral microbleeds; CSO = centrum semiovale; dPVS = dilated perivascular spaces; MMSE = Mini-Mental State Examination; NA = all patients with large infarct had stroke; PVH = periventricular WMH; WMH = white matter hyperintensities.
Association between each inventory tool item and the different clinical outcomes; the analysis was performed separately for each item (model 1, significance at *$p < 0.0045$).
Association between inventory tool item and the different clinical outcomes independently from the other items (model 2, multivariate analysis, significance at ***$p < 0.001$; **$p < 0.01$, #$p < 0.05$). The total scores are not included in model 2 to avoid collinearity with the raw items.
Values in bold represent significant positive association between inventory tool scores and clinical outcomes, while values in italic and with underline represent significant negative association.

Figure 4 Illustrative Cases Showing Different Scores Derived From the Inventory Tool Obtained From Various Images

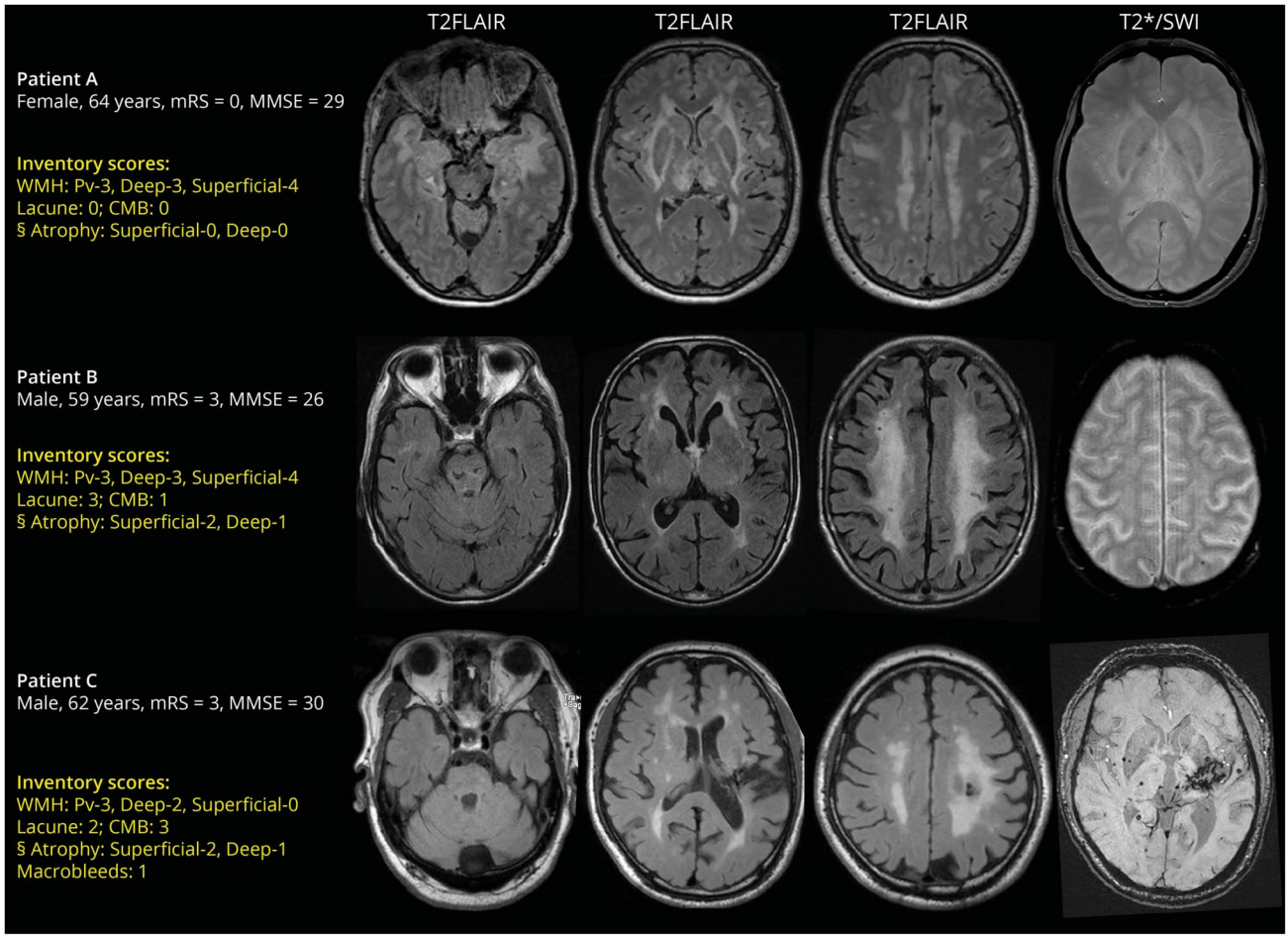

Patient A: A 64-year-old woman, with predominantly superficial WMH (PVH, deep WMH, and superficial WMH scores = 3, 3, and 4, respectively) but no lacune, CMB, or atrophy. She had no stroke history, mRS = 0 and MMSE = 29. Patient B: A 59-year-old man, with predominantly periventricular WMH (PVH, deep WMH, and superficial WMH scores = 3, 3, and 0, respectively), more than 10 lacunes (lacune score = 3), and significant brain atrophy (superficial and deep atrophy scores = 2, 1, respectively). He had stroke history, with mRS = 3 and MMSE = 26. Patient C: A 62-year-old man, from cohort 3, with moderate PVH and deep WMH and no superficial WMH (PVH, deep WMH, and superficial WMH score = 3, 2, and 0, respectively), more than 30 CMB (CMB score = 3), 1 macrobleed and significant brain atrophy (superficial and deep atrophy score = 2 and 1, respectively). He had stroke history, with mRS = 3 and MMSE = 30. [§]3D T1 was used for assessment but not shown. CMB = cerebral microbleed; FLAIR = fluid-attenuated inversion recovery; MMSE = Mini-Mental State Examination; mRS = modified Rankin scale; Pv = periventricular; PVH = periventricular WMH; SWI = susceptibility-weighted imaging; WMH = white matter hyperintensity.

0.556), and the dPVS items especially when they were obtained using the basic MRI protocol based on low-resolution images (interrater: weighted κ between 0.211 and 0.256; intrarater: 0.388–0.589).

Correlations Between the Items From the Inventory Tool and Quantifications of Lesions

PVH, deep WMH, and superficial WMH items were correlated with each other (PVH and deep WMH: Pearson r = 0.645, $p < 0.001$; PVH and superficial WMH: Pearson r = 0.399, $p < 0.001$; deep WMH and superficial WMH: Pearson $r = 0.425$, $p < 0.001$). The correlation between the WMH total score, calculated by summing the previous scores, and the cube root of WMH fraction was high in all 3 cohorts (cohort 1: Pearson $r = 0.792$, $p < 0.001$; cohort 2: Pearson $r = 0.897$, $p < 0.001$; cohort 3: Pearson $r = 0.877$, $p < 0.001$; all patients: Pearson $r = 0.833$, $p < 0.001$) (Figure 3A).

Superficial atrophy and deep atrophy items were correlated with each other (Pearson $r = 0.712$, $p < 0.001$). The atrophy total score was correlated with the normal quantile-transformed BPF in all 3 cohorts (cohort 1: Pearson $r = -0.753$, $p < 0.001$; cohort 2: Pearson $r = -0.617$, $p < 0.001$; cohort 3: Pearson $r = -0.572$, $p < 0.001$; all patients: Pearson $r = -0.707$, $p < 0.001$) (Figure 3B).

Association Between the Inventory Tool Scores and the Main Clinical Features of the Disease

The results of the association analysis between the different inventory tool items and the clinical variables are summarized in Table 3. In the first model, stroke was positively associated with the WMH scores, lacunes, and CMB scores but negatively associated with the CSO dPVS score. Migraine with aura was positively associated with the superficial WMH score but negatively associated with the CMB and superficial

atrophy scores. Disability was positively associated with the PVH, deep WMH, lacune, CMB, and atrophy scores but negatively associated with the CSO dPVS score. Lower MMSE was positively associated with the PVH, lacune, CMB, and atrophy scores but negatively associated with the CSO dPVS score.

When all items were considered together (model 2) for analysis, the results showed that scores of lacunes and macrobleeds were positively associated with stroke. CMB and superficial atrophy scores were negatively associated with migraine with aura, while deep atrophy score was positively associated with migraine with aura. PVH, lacune, superficial atrophy scores, large infarct, and macrobleeds were positively associated with disability. Higher PVH, deep WMH, and atrophy and macrobleed scores were associated with lower MMSE.

Finally, the models based on a combination of items derived from the inventory tool (Table 3) largely outperform those obtained using a global score as the CSVD total score for predicting the different clinical outcomes. Not only the R^2 was found always higher using items from CADA-MRIT but also 2 major clinical outcomes, migraine with aura and the MMSE score, were associated with scores derived from our tool but not with the total CSVD score (eTable 3, links.lww.com/WNL/D94).

Time-Effectiveness

As summarized in eTable 4 (links.lww.com/WNL/D94), the mean time for using the inventory tool for assessing MRI data from a patient with CADASIL was approximately 2–3 minutes. The mean time needed for evaluating images obtained using an advanced MRI protocol including 3D MRI data was 50 seconds longer than with images obtained using the basic MRI protocol. The most time-consuming items were the lacunes and the dPVS.

Discussion

In this study, we have developed and evaluated an easy-to-use imaging inventory tool for analyzing and comparing the most frequent MRI lesions observed in CADASIL across different cohorts or populations. This tool was developed based on data from 3 independent cohorts originating from Europe and Asia. The results showed that this instrument was not only reliable but could also be used with different imaging sequences and provides scores that were clinically relevant, all this in a very short time for completion.

This tool was designed to obtain a multifaceted assessment of cerebral MRI lesions in CADASIL, not to quantify a single imaging marker as proposed through different visual rating scales available in the literature. The inventory tool allows for evaluating the extent of the most characteristic imaging features observed in patients with CADASIL, that is, not only WMH, lacunes, and microbleeds but also cerebral atrophy and the presence of large infarcts or large hemorrhages. All these markers have been repeatedly shown to vary considerably according to the progression of the disease and to be differently related to the clinical severity.[4,18] The results showed that its use allowed to detect easily the high frequency of hemorrhagic lesions and rarity of temporal damage in the Taiwanese cohort (cohort 3) in contrast to the 2 other cohorts (Figure 4).[32] This is exactly one of the possible uses of such a tool, which might be also used for evaluating in future the influence of vascular risk factors, locations of the *NOTCH3* sequence variant, or even additional genetic variants on the multiple imaging manifestations of the disease.

The results we obtained from different angles showed that this inventory tool was highly reliable. First, the items derived from the inventory were strongly correlated when images were acquired using different MRI sequences. These results are important because they suggest that the levels of items taken from this inventory in different centers and cohorts could be actually compared. Second, we observed that these imaging items were strongly related to the quantitative measures of lesions obtained using various algorithms and multiple data preparation steps. This demonstration was obtained after summing the different items of hyperintensities in the periventricular, deep, and superficial white matter that we compared with the global volumetric measures of lesions. Identical results were obtained after summing the superficial and deep atrophy items that we compared with the BPF. These results also suggest that such global scores of WMH or atrophy derived from the inventory tool could also be considered for estimating the total amount of white matter lesions or degree of cerebral atrophy across CADASIL patient groups. Elsewhere, because the rating of white matter lesions was developed from items originating from the long-validated Fazekas scale, the 2 subscores of the latter could be easily retrieved by only changing the PVH level 4 in level 3 in the inventory tool. Third, the different items derived from the inventory were also highly reproducible. For most of them, a high interrater and intrarater agreement was reached, which supports that the inventory tool could be used by multiple observers and repeatedly when needed. These results were, however, obtained with MRI read by experienced neurologists or neuroradiologists and would need further evaluation for other categories of readers. Our experience during the study suggested, however, that meeting before the first evaluation for discussing how to use the method in detail, evaluating approximately 10 cases in common, and using a clear illustration of rating as shown in Figure 2 were presumably crucial to reach highly reproducible items. As expected with experiencing the method during the study, only the rating of dPVS did not reach a high level of interrater agreement, particularly when using images from basic MRI protocols without T2 images or low-resolution data from 1.5T MRI. This was not surprising insofar because dPVS were the finest signal abnormalities to be detected on MRI.[33] Thus, the quality of detection depended not only on the possibility to follow the corresponding vascular trajectories in 3D but also on the level

of image resolution as already illustrated using extreme resolution with 7.0T MRI.[34,35]

The analysis of the association between the different imaging items and the main clinical manifestations of the disease showed results in perfect agreement with different links already established between quantitative MRI markers and the clinical severity in CADASIL. The significant association between stroke and the score of lacunes or that of macrobleeds, which was not found with WMH items, has been previously reported by measuring the load of lacunes and total volume of WMH.[9,32] In addition, the independent association between disability or MMSE score with the lacune and atrophy items are in line with previous reports showing that the accumulation of lacunes was not only a key driver of motor and cognitive decline during the progression of CADASIL but also promoted the development of cerebral and cortical atrophy.[36-38] Finally, the association observed with the PVH item but not with the superficial WMH item is in agreement with the different types of white matter lesions of distinct nature and clinical impact already delineated in CADASIL.[12,39] Of interest, we observed that migraine with aura was negatively correlated with superficial atrophy and possibly related to WMH in the temporal lobes. Further analyses are needed to better understand the potential clinical links between lesions in the temporal white matter relatively specific to the disease.[40,41] Of interest, although our tool was not primarily developed to reflect the clinical severity of the disease in terms of brain damage, scores that could be derived from our tool might also provide crucial information about the brain lesions variably associated with different clinical manifestations of the disease. Our results clearly showed that the CADA-MRIT items allowed, in any case, to predict the different clinical manifestations of CADASIL better than the use of a simple and global score as the total CSVD score developed in another context and for different purposes.[31]

Obviously, this study based on the development and validation of a specific tool to inventory multiple categories of MRI lesions in CADASIL presents many strengths. This tool was proposed based on a real need to compare easily and quickly patients' imaging data across countries or cohorts. It was developed both by CADASIL and MRI experts of CSVD from data collected from more than 600 individuals and 3 distinct cohorts with a large spectrum of clinical and cerebral manifestations. Its reliability was extensively assessed from multiple angles, and the derived imaging items were found clinically relevant. The tool was particularly easy to use and fast and could provide directly different imaging items at the patient bed and for clinical research. Based on this inventory, a rapid and more massive combination of data could be envisaged in future research. Some refinements could certainly improve it further for investigating other rare CSVD or answering very specific questions. For example, lacunes in the pons could be added as an additional item when evaluating pontine autosomal dominant microangiopathy and leukoencephalopathy.[42] The location of lacunes or microbleeds, which was not assessed in the inventory, would also need additional items. We are also aware of some limitations of such an approach. Although we compiled different imaging protocols for validating the reproducibility of the inventory tool, we could not ascertain that other parameters from other MRI sequences not used in this study could not influence the different imaging items. In addition, the method can in no way be used to assess the progression of the disease over a limited time frame. In addition, it does not provide any continuous measure, which limits the statistical power for detecting small differences. The evaluation of lesions remains also dependent on the quality of data and resolution of images, particularly for PVS. Moreover, because the different items of the inventory tool were variously associated with the clinical manifestations of the disease, we could not provide immediately a "total score" of lesions related to the clinical progression of the disease from this inventory. The weights of its multiple items might be probably adjusted in future to obtain a global score of severity according to the aim and design of future studies. In the meantime, the results from our inventory can be easily transformed to the CSVD total score[31] or to the Fazekas score[20] when seeking for a simple comparison with the burden of lesions assessed in other databases or small vessel diseases.

In conclusion, we believe that the inventory tool developed and validated in this study is a new instrument for CADASIL research. It should first greatly facilitate the common assessment of large amounts of brain imaging data and comparison between cohorts and multiple samples of patients. Further studies will be needed to determine how this tool could be also used to facilitate the instant evaluation of patients at bedside, prognostication, and triage for future therapeutic trials in CADASIL.

Acknowledgment

The authors thank the team in charge of formatting and cleaning the database using multiple information collected over 14 years from different sources and which made possible this study, particularly Professor Sylvie Chevret and Mrs. Claire Pacheco (INSERM UMR1136). The authors thank Dr. Dominique Hervé and Nassira Alili who collected important clinical data for this study, Mr. Abbas Taleb for collecting most of information along the cohort study, Mrs. Sonia Reyes who is responsible for neuropsychological assessments, Mrs. Aude Jabouley and Carla Machado who performed a large number of cognitive evaluation in the cohort, Mrs. Solange Hello who managed and organized the appointment of multiple family members involved in the study, and Mrs. Nathalie Dias-Gastelier and Fanny Fernandes, the research managers in charge of the Cohort Study. The authors thank the CADASIL France Association for their help and permanent support.

Study Funding

R. Zhang is funded by the China Postdoctoral Council (grant no. PC2020117) and the National Natural Science Foundation of China (grant no. 82101987). S.-C. Tang is supported by the grant from the National Science and Technology Council (NSTC) Taiwan (110-2314-B-002-155-MY3). H.

Chabriat is supported by grants from the French Ministry of Health (Regional and National PHRC AOR 02-001) and Research (Agence National de la Recherche, ANR, RHU TRT_cSVD), Association de Recherche en NEurologie VAsculaire.

Disclosure

The authors report no disclosures relevant to the manuscript. Go to Neurology.org/N for full disclosures.

Publication History

Received by *Neurology* March 7, 2023. Accepted in final form June 12, 2023. Submitted and externally peer reviewed. The handling editor was Editor-in-Chief José Merino, MD, MPhil, FAAN.

Appendix Authors

Name	Location	Contribution
Ruiting Zhang, MD, PhD	Paris-Cité University, Inserm U1141 NeuroDiderot, France; Department of Radiology, the Second Affiliated Hospital of Zhejiang University, School of Medicine, Hangzhou, China	Drafting/revision of the article for content, including medical writing for content; study concept or design; and analysis or interpretation of data
Chih-Hao Chen, MD, PhD	Department of Neurology, National Taiwan University Hospital, Taipei; Department of Clinical Neurosciences, University of Calgary, Alberta, Canada	Drafting/revision of the article for content, including medical writing for content; major role in the acquisition of data
Sophie Tezenas Du Montcel, MD, PhD	Sorbonne Université, INSERM, Unité Mixte de Recherche 1136, Institut Pierre Louis d'Épidémiologie et de Santé Publique; Sorbonne Université, INSERM, Institut Pierre Louis d'Épidémiologie et de Santé Publique, AP-HP, Hôpitaux Universitaires Pitié Salpêtrière–Charles Foix, Paris, France	Drafting/revision of the article for content, including medical writing for content; and analysis or interpretation of data
Jessica Lebenberg, PhD	Paris-Cité University, Inserm U1141 NeuroDiderot; Lariboisière University Hospital, APHP, Translational Neurovascular Centre and Department of Neurology, Reference Center for Rare Vascular Diseases of the Central Nervous System and the Retina (CERVCO), FHU NeuroVasc, Paris, France	Drafting/revision of the article for content, including medical writing for content; major role in the acquisition of data
Yu-Wen Cheng, MD, PhD	Department of Neurology, National Taiwan University Hospital, Taipei; Department of Neurology, National Taiwan University Hospital Hsinchu Branch, Hsinchu	Drafting/revision of the article for content, including medical writing for content; major role in the acquisition of data
Martin Dichgans, MD, PhD	Institute for Stroke and Dementia Research, University Hospital, Ludwig Maximilian University; German Center for Neurodegenerative Diseases (DZNE), Munich; Munich Cluster for Systems Neurology (SyNergy), Germany	Drafting/revision of the article for content, including medical writing for content; major role in the acquisition of data
Sung-Chun Tang, MD, PhD	Department of Neurology, National Taiwan University Hospital, Taipei	Drafting/revision of the article for content, including medical writing for content; major role in the acquisition of data
Hugues Chabriat, MD, PhD	Paris-Cité University, Inserm U1141 NeuroDiderot; Lariboisière University Hospital, APHP, Translational Neurovascular Centre and Department of Neurology, Reference Center for Rare Vascular Diseases of the Central Nervous System and the Retina (CERVCO), FHU NeuroVasc, Paris, France	Drafting/revision of the article for content, including medical writing for content; major role in the acquisition of data; study concept or design; and analysis or interpretation of data

References

1. Chabriat H, Joutel A, Dichgans M, Tournier-Lasserve E, Bousser MG. Cadasil. *Lancet Neurol*. 2009;8(7):643-653. doi:10.1016/s1474-4422(09)70127-9
2. Opherk C, Peters N, Herzog J, Luedtke R, Dichgans M. Long-term prognosis and causes of death in CADASIL: a retrospective study in 411 patients. *Brain*. 2004;127(11):2533-2539. doi:10.1093/brain/awh282
3. Zhang R, Ouin E, Grosset L, et al. Elderly CADASIL patients with intact neurological status. *J Stroke*. 2022;24(3):352-362. doi:10.5853/jos.2022.01578
4. Gravesteijn G, Hack RJ, Opstal AMV, et al. Eighteen-year disease progression and survival in CADASIL. *J Stroke*. 2021;23(1):132-134. doi:10.5853/jos.2020.04112
5. Rutten JW, Van Eijsden BJ, Duering M, et al. The effect of NOTCH3 pathogenic variant position on CADASIL disease severity: NOTCH3 EGFr 1-6 pathogenic variant are associated with a more severe phenotype and lower survival compared with EGFr 7-34 pathogenic variant. *Genet Med*. 2019;21(3):676-682. doi:10.1038/s41436-018-0088-3
6. Hack RJ, Gravesteijn G, Cerfontaine MN, et al. Three-tiered EGFr domain risk stratification for individualized NOTCH3-small vessel disease prediction. *Brain*. 2022,146(7):2913-2927. doi:10.1093/brain/awac486
7. Adib-Samii P, Brice G, Martin RJ, Markus HS. Clinical spectrum of CADASIL and the effect of cardiovascular risk factors on phenotype: study in 200 consecutively recruited individuals. *Stroke*. 2010;41(4):630-634. doi:10.1161/strokeaha.109.568402
8. Ciolli L, Pescini F, Salvadori E, et al. Influence of vascular risk factors and neuropsychological profile on functional performances in CADASIL: results from the MIcrovascular LEukoencephalopathy Study (MILES). *Eur J Neurol*. 2014;21(1):65-71. doi:10.1111/ene.12241
9. Chabriat H, Herve D, Duering M, et al. Predictors of clinical worsening in cerebral autosomal dominant arteriopathy with subcortical infarcts and leukoencephalopathy: prospective cohort study. *Stroke*. 2016;47(1):4-11. doi:10.1161/strokeaha.115.010696
10. Ni W, Zhang Y, Zhang L, Xie JJ, Li HF, Wu ZY. Genetic spectrum of NOTCH3 and clinical phenotype of CADASIL patients in different populations. *CNS Neurosci Ther*. 2022;28(11):1779-1789. doi:10.1111/cns.13917
11. Kim Y, Bae JS, Lee JY, et al. Genotype and phenotype differences in CADASIL from an Asian perspective. *Int J Mol Sci*. 2022;23(19):11506. doi:10.3390/ijms231911506
12. De Guio F, Vignaud A, Chabriat H, Jouvent E. Different types of white matter hyperintensities in CADASIL: insights from 7-Tesla MRI. *J Cereb Blood Flow Metab*. 2018;38(9):1654-1663. doi:10.1177/0271678x17690164
13. Kuijf HJ, Biesbroek JM, De Bresser J, et al. Standardized assessment of automatic segmentation of white matter hyperintensities and results of the WMH segmentation challenge. *IEEE Trans Med Imaging*. 2019;38(11):2556-2568. doi:10.1109/tmi.2019.2905770
14. Lebenberg J, Guichard JP, Guillonnet A, et al. The epidermal growth factor domain of the mutation does not appear to influence disease progression in CADASIL when brain volume and sex are taken into account. *AJNR Am J Neuroradiol*. 2022;43(5):715-720. doi:10.3174/ajnr.a7499
15. Cheng AL, Batool S, McCreary CR, et al. Susceptibility-weighted imaging is more reliable than T2*-weighted gradient-recalled echo MRI for detecting microbleeds. *Stroke*. 2013;44(10):2782-2786. doi:10.1161/strokeaha.113.002267
16. Chen CH, Chu YT, Chen YF, et al. Comparison of clinical and neuroimaging features between NOTCH3 mutations and nongenetic spontaneous intracerebral haemorrhage. *Eur J Neurol*. 2022;29(11):3243-3254. doi:10.1111/ene.15485
17. Viswanathan A, Guichard JP, Gschwendtner A, et al. Blood pressure and haemoglobin A1c are associated with microhaemorrhage in CADASIL: a two-centre cohort study. *Brain*. 2006;129(9):2375-2383. doi:10.1093/brain/awl177
18. Ling Y, De Guio F, Jouvent E, et al. Clinical correlates of longitudinal MRI changes in CADASIL. *J Cereb Blood Flow Metab*. 2019;39(7):1299-1305. doi:10.1177/0271678x18757875
19. Rutten JW, Hack RJ, Duering M, et al. Broad phenotype of cysteine-altering NOTCH3 variants in UK Biobank: CADASIL to nonpenetrance. *Neurology*. 2020;95(13):e1835-e1843. doi:10.1212/wnl.0000000000010525

20. Fazekas F, Chawluk JB, Alavi A, Hurtig HI, Zimmerman RA. MR signal abnormalities at 1.5 T in Alzheimer's dementia and normal aging. *AJR Am J Roentgenol*. 1987; 149(2):351-356. doi:10.2214/ajr.149.2.351
21. Gregoire SM, Chaudhary UJ, Brown MM, et al. The Microbleed Anatomical Rating Scale (MARS): reliability of a tool to map brain microbleeds. *Neurology*. 2009;73(21): 1759-1766. doi:10.1212/wnl.0b013e3181c34a7d
22. Zhu YC, Tzourio C, Soumaré A, Mazoyer B, Dufouil C, Chabriat H. Severity of dilated Virchow-Robin spaces is associated with age, blood pressure, and MRI markers of small vessel disease: a population-based study. *Stroke*. 2010;41(11):2483-2490. doi: 10.1161/strokeaha.110.591586
23. Doubal FN, MacLullich AM, Ferguson KJ, Dennis MS, Wardlaw JM. Enlarged perivascular spaces on MRI are a feature of cerebral small vessel disease. *Stroke*. 2010; 41(3):450-454. doi:10.1161/strokeaha.109.564914
24. Mäntylä R, Erkinjuntti T, Salonen O, et al. Variable agreement between visual rating scales for white matter hyperintensities on MRI. Comparison of 13 rating scales in a poststroke cohort. *Stroke*. 1997;28(8):1614-1623. doi:10.1161/ 01.str.28.8.1614
25. Harper L, Barkhof F, Fox NC, Schott JM. Using visual rating to diagnose dementia: a critical evaluation of MRI atrophy scales. *J Neurol Neurosurg Psychiatry*. 2015;86(11): 1225-1233. doi:10.1136/jnnp-2014-310090
26. Cordonnier C, Potter GM, Jackson CA, et al. Improving interrater agreement about brain microbleeds: development of the Brain Observer MicroBleed Scale (BOMBS). *Stroke*. 2009;40(1):94-99. doi:10.1161/strokeaha.108.526996
27. Taniguchi A, Shindo A, Tabei KI, et al. Imaging characteristics for predicting cognitive impairment in patients with cerebral autosomal dominant arteriopathy with subcortical infarcts and leukoencephalopathy. *Front Aging Neurosci*. 2022;14:876437. doi: 10.3389/fnagi.2022.876437
28. Dupe C, Guey S, Biard L, et al. Phenotypic variability in 446 CADASIL patients: impact of NOTCH3 gene mutation location in addition to the effects of age, sex and vascular risk factors. *J Cereb Blood Flow Metab*. 2023;43(1):153-166. doi:10.1177/ 0271678x221126280
29. Cheng YW, Chao CC, Chen CH, et al. Small fiber pathology in CADASIL: clinical correlation with cognitive impairment. *Neurology*. 2022;99(6):e583-e593. doi: 10.1212/wnl.0000000000200672
30. Landis JR, Koch GG. The measurement of observer agreement for categorical data. *Biometrics*. 1977;33(1):159-174. doi:10.2307/2529310
31. Staals J, Makin SD, Doubal FN, Dennis MS, Wardlaw JM. Stroke subtype, vascular risk factors, and total MRI brain small-vessel disease burden. *Neurology*. 2014;83(14): 1228-1234. doi:10.1212/wnl.0000000000000837
32. Chen CH, Tang SC, Cheng YW, et al. Detrimental effects of intracerebral haemorrhage on patients with CADASIL harbouring NOTCH3 R544C mutation. *J Neurol Neurosurg Psychiatry*. 2019;90(7):841-843. doi:10.1136/jnnp-2018-319268
33. Pham W, Lynch M, Spitz G, et al. A critical guide to the automated quantification of perivascular spaces in magnetic resonance imaging. *Front Neurosci*. 2022;16:1021311. doi:10.3389/fnins.2022.1021311
34. Huang P, Zhang R, Jiaerken Y, et al. Deep white matter hyperintensity is associated with the dilation of perivascular space. *J Cereb Blood Flow Metab*. 2021;41(9): 2370-2380. doi:10.1177/0271678x211002279
35. Lian C, Zhang J, Liu M, et al. Multi-channel multi-scale fully convolutional network for 3D perivascular spaces segmentation in 7T MR images. *Med Image Anal*. 2018;46: 106-117. doi:10.1016/j.media.2018.02.009
36. Viswanathan A, Gschwendtner A, Guichard JP, et al. Lacunar lesions are independently associated with disability and cognitive impairment in CADASIL. *Neurology*. 2007;69(2):172-179. doi:10.1212/01.wnl.0000265221.05610.70
37. Viswanathan A, Godin O, Jouvent E, et al. Impact of MRI markers in subcortical vascular dementia: a multi-modal analysis in CADASIL. *Neurobiol Aging*. 2010;31(9): 1629-1636. doi:10.1016/j.neurobiolaging.2008.09.001
38. Jouvent E, Viswanathan A, Mangin JF, et al. Brain atrophy is related to lacunar lesions and tissue microstructural changes in CADASIL. *Stroke*. 2007;38(6):1786-1790. doi: 10.1161/strokeaha.106.478263
39. Duchesnay E, Hadj Selem F, De Guio F, et al. Different types of white matter hyperintensities in CADASIL. *Front Neurol*. 2018;9:526. doi:10.3389/fneur.2018.00526
40. De Guio F, Mangin JF, Duering M, Ropele S, Chabriat H, Jouvent E. White matter edema at the early stage of cerebral autosomal-dominant arteriopathy with subcortical infarcts and leukoencephalopathy. *Stroke*. 2015;46(1):258-261. doi:10.1161/strokeaha.114.007018
41. De Guio F, Germanaud D, Lefevre J, et al. Alteration of the cortex shape as a proxy of white matter swelling in severe cerebral small vessel disease. *Front Neurol*. 2019;10: 753. doi:10.3389/fneur.2019.00753
42. Ding XQ, Hagel C, Ringelstein EB, et al. MRI features of pontine autosomal dominant microangiopathy and leukoencephalopathy (PADMAL). *J Neuroimaging*. 2010; 20(2):134-140. doi:10.1111/j.1552-6569.2008.00336.x

Additional eReferences are listed at links.lww.com/WNL/D95.